Evaluation of mixing and chemical reactions within a jet in crossflow by means of LES

J. A. Denev, J. Fröhlich and H. Bockhorn*
Institute for Technical Chemistry and Polymer Chemistry, University of Karlsruhe (TH)
Kaiserstrasse 12, 76128 Karlsruhe, Germany

Abstract
The mixing processes for the configuration of a jet in crossflow are studied by means of Large Eddy Simulation (LES). The species are regarded as passive scalars, two of them are reacting. The study has been performed with both turbulent and laminar inflow conditions in the pipe (at the same Re number) exhibiting quite different results for the two regimes. Different mixing indices are computed to quantify the mixing in planes perpendicular to the crossflow. Principal difficulties arising from the choice of the integration area for the mixing indices are discussed. Areas of high reaction rate are found to correlate well with areas of high turbulent kinetic energy.

Introduction

The configuration of a transverse jet into a crossflow has been frequently investigated both numerically and experimentally since more than 50 years. These research activities are justified for two reasons: first, the jet in crossflow is widely used in applications with mixing and combustion such as, e.g., power plant technology; second, this flow configuration exhibits a complex vortex structure which is still not fully understood. While the majority of investigations are concerned with the flow field alone, there are less numerical investigations on mixing and even fewer on chemical reactions. The present study focuses on the mixing process of both reacting and non-reacting scalars.

In a previous paper [1] the mixing of a passive scalar for the same geometry and flow conditions (velocity ratio 3.3) has been studied by the present authors. Results for the average scalar concentration and the scalar fluctuations of a passive scalar issued from the jet pipe have been compared with results from other authors. Good agreement with both experimental data and LES reported in [2,3] have been achieved. The effect of using different values of the Smagorinsky constant or the Dynamic Smagorinsky Model have been quantified showing that there is not a clear superiority of any of these approaches.

In the present paper a slightly different approach to investigating of the mixing capacity of the flow is chosen. The new feature is that also a simple chemical reaction is considered. While the concentration of the species is always influenced by the (convective) history of the upstream flow, the reaction rate monitors the local mixing phenomena. In the present study average reaction rate and turbulent fluctuations of the reaction rate are recorded and are used, together with the corresponding instantaneous values, for the analysis of the mixing flow phenomena. It is shown that locations of intensive mixing and reaction coincide with particular vortex structures in the flow, the spanwise rollers and the hanging vortices.

The specific objective of the present study is to get insight into the mixing phenomena of a jet in crossflow by the following means:

- Analysis of mixing indices for non-reacting scalars.
- Analysis of a one-step chemical reaction and the correlation of the reaction rate and the turbulence characteristics of the flow.
- Identification of regions of high reaction rates and high concentrations of the reacting scalars.

Additional objectives are:

- To evaluate the importance of proper turbulent boundary conditions in the jet-pipe.
- To investigate the quality of the numerical grid in respect to the needs of modelling the reaction term for the concentration equation of the reacting scalars.

Flow studied and computational method

The simulations were conducted for a jet emitted from a circular pipe at 90 degrees into a laminar crossflow, as previously studied in [1,2,3]. The Reynolds number based on the jet diameter D and the jet velocity U_{jet} is 6930 and the velocity ratio is U_{jet}/U_{cross}=3.3. The computational domain extends over x=-2.7…11.5D, y=-4…4D, z=-1…12D in stream-wise, spanwise and wall-normal direction, respectively, with the centre of the outlet located at the origin. All lengths and velocities are made non-dimensional with D and U_{cross}, respectively. The velocity boundary condition for the crossflow was steady at the inlet featuring a Blasius profile of thickness 0.5D. Turbulent inflow in the pipe at z=-D was generated by a precursor simulation of developed pipe flow with periodic conditions and a length of 5D. For comparison, laminar pipe flow was also considered imposing a parabolic profile at z=-D.

The filtered Navier-Stokes equations for incompressible fluid were solved with the collocated, curvilinear, block-structured Finite Volume code LESOCC2 [4] using central second order schemes in

* Corresponding author: denev@ict.uni-karlsruhe.de
Associated Web site: http://www.ict.uni-karlsruhe.de/index.pl/themen/dns/index.html
Proceedings of the European Combustion Meeting 2005

space for all fluxes and a second order Runge-Kutta scheme in time. The Smagorinsky model was employed for subgrid-scale modelling with Cs=0.1 and the Werner-Wengle wall model [5] at all solid boundaries. Due to its inherent blending this approach reduces to a no-slip condition in the laminar case.

The grid employed consists of 50 blocks with 1.9 Mio cells, 440000 of which are located in the precursor domain. A slip condition was used at y=+-4D and a convective condition at the outlet. All simulations were pursued over substantial time accumulating statistical data over 100 dimensionless time units.

The mixing of the jet with the crossflow was investigated in two steps. In the first step, a non-reactive passive scalar S_1 was introduced with concentration Y_1=1 in the pipe and Y_1=0 in the crossflow. Micro-mixing was modelled analogously to the velocity subgrid-scale model by a turbulent Schmidt number of 0.6, while the molecular Schmidt number was Sc=0.7 for all species.

In the second step, two reactive scalars A and B were introduced with the same boundary conditions as S_1 and S_2. They react in an idealized irreversible isothermal one-step reaction according to 1A + 1B → 1P. The reaction rate ω was modeled as $\omega = Da\, Y_A Y_B$, where Y_A and Y_B are the mass fractions of species A and B, respectively. The Damköhler number Da was set equal to 1, i.e. the reaction is relatively slow, so that the time scales for the turbulence and for the chemical reaction are equal. With the present approach, the reaction rate is computed from the filtered mass fractions only. In [6] this approach is termed the "resolved reaction rate model" (RRRM) with *a priori* tests in this reference revealing that the reaction rate was over-predicted compared to DNS. The modeling error, however, strongly depends on the coarseness of the grid. Using the turbulent viscosity as "grid coarseness" criterion as discussed below shows that the numerical grid employed in the present study is relatively fine in locations where the reaction rate is high, so that with Da=1 the results obtained with this model should be reasonably accurate and provide useful qualitative information.

Results and Discussion

Influence of the flow regime. The Reynolds number of the pipe flow, based on pipe velocity and diameter, is higher than the critical one (Re = 6930 > $Re_{crit} \approx 2300$). However, from a numerical point of view it is much easier to construct boundary conditions for a laminar case than for a turbulent one (see above). Therefore, one aim was to evaluate the influence of the inlet flow regime on the jet. Fig. 1 shows a comparison of the jet trajectory for the two cases. The Reynolds number was the same in both cases, but the inflow condition was changed from the turbulent one described above to a steady parabolic profile. The jet trajectory in each case was calculated from the averaged flow as the streamline starting from the center point of the inlet with coordinates (0,0,0). Fig. 1 shows that the difference between the two cases is substantial. At a distance of x=10D, e.g., the turbulent jet is about 1.7D lower than the laminar one. This is due to the increased exchange of momentum between jet and crossflow in the case of a turbulent jet.

With laminar jet inflow condition, a recirculation zone is observed in the pipe along the upstream section of the wall which reaches down to z=-0.4D. Consequently, crossflow fluid carrying the scalar B is observed here. In the computations with reactive scalars this lead to substantial reaction rate in the pipe prior to the outlet which is absent in the case of turbulent inlet conditions.

The observations just reported demonstrate that the additional efforts to calculate the turbulent pipe flow using periodic boundary conditions were justified. In the sequel, only results obtained with turbulent jet flow will be presented.

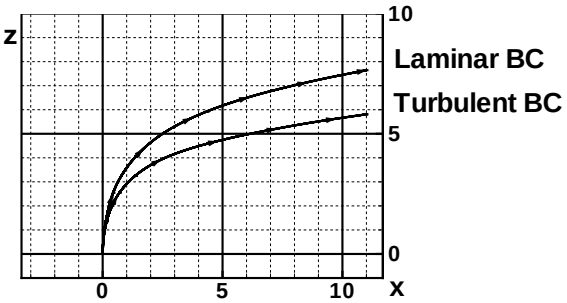

Fig. 1. Comparison of the middle jet trajectory for laminar and turbulent jet flow, imposed in the pipe 1D upstream of the outlet into the crossflow. The pipe is not shown in the figure.

Non-reacting scalars and mixing indices. A large variety of indices quantifying mixing processes are available in the literature. Boss [7] counted 37 different definitions. Following the work of Prière et al. [8] who investigated a series of jets in crossflow, the Temporal Mixing Deficiency (TMD) is used here to evaluate the quality of mixing at successive downstream locations of the flow. It is defined as

$$TMD = Avg\left(\frac{\sqrt{<Y_1'Y_1'>}}{<Y_1>}\right)\times 100[\%] \quad . \qquad (1)$$

Variables like $<Y_1'Y_1'>$ and $<Y_1>$ which present the time-averaged scalar fluctuations and the time-averaged concentration for scalar S_1 are obtained directly from the LESOCC2 code at the end of the computations. In Eq. (1), "Avg" stands for the spatial average taken over all points in a characteristic plane. Here, a principal problem connected with the configuration of a jet in crossflow becomes evident:

- the relative fluctuations, inside the round brackets, are undefined if the denominator in Eq. (1) is zero;
- the natural choice for the averaging area, the cross-section of the crossflow-channel includes points outside the jet with $<Y_1>=0$. Furthermore, points where the average concentration is small but still positive dominate the averaged value.

These issues concern both numerical and experimental studies.

In order to overcome the above difficulties, the following approach is suggested here: the area of averaging is set according to a threshold for the concentration $< Y_1 >$, or, in other words the area is defined as locations where:

$$<Y_1> \; > \; <Y_1>_{treshold} \cdot \qquad (2)$$

The additional question arises about how sensitive the TMD index is relative to the value of $< Y_1 >_{treshold}$. This is addressed by choosing the threshold value equal to 1.0, 2.5, 5.0 and 10% of the inlet value of S_1 in the pipe. Fig. 2 presents the resulting averaging area, defined by the four values.

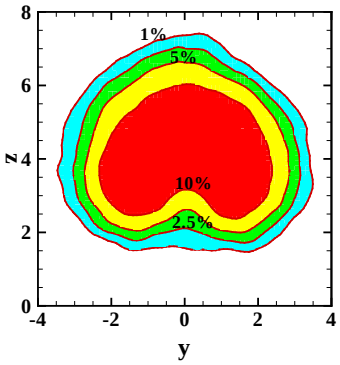

Fig. 2. The averaging area for determining the TMD of S_1 at x/D=9 using the four different thresholds mentioned in the text.

The TMD decreases in value when the mixing increases and vanishes for a perfectly mixed fluid. For the present flow configuration it is expected to decrease monotonically as one moves downstream with the crossflow. Figure 3 shows the values of this index for planes with increasing x/D coordinate and for the averaging thresholds listed before.

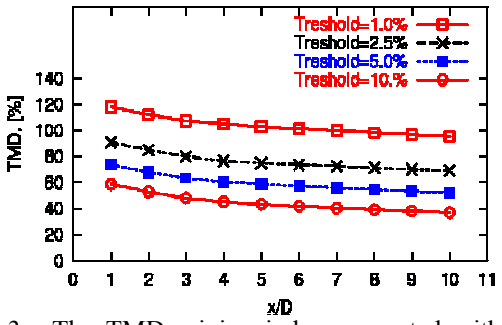

Fig. 3. The TMD mixing index computed with four different values of the area-defining threshold.

It turns out that the absolute value of the index is quite sensitive to the choice of the threshold used for the definition of the averaging area. Figure 3 shows a reduction of the TMD with increasing threshold. This results from large values of the index in the peripheral zones of the jet which are generated by the high intermittency of the scalar in these zones. On the other hand, the decay of all curves in Fig. 3 with increasing distance x/D is extremely similar. This allows to obtain reliable information about the mixing improvement between planes with different x/D coordinates. All four curves in Fig. 3, e.g., show that between x/D=1 and x/D=10 the TMD indicates an improvement of mixing by 20%.

Other indices presented in [8] have been computed as well for the present configuration, such as the Spatial Mixing Deficiency (SMD)

$$SMD = \frac{RMS(< Y_1 > - Avg(< Y_1 >))}{Avg(< Y_1 >)} \times 100[\%] \quad , \qquad (3)$$

where again "Avg" denotes spatial averaging and "RMS" the root-mean-square in the spatial sense. These indices however exhibit even higher sensitivity with respect to the threshold value for the jet in crossflow configuration as exemplified by the SMD in Fig. 4.

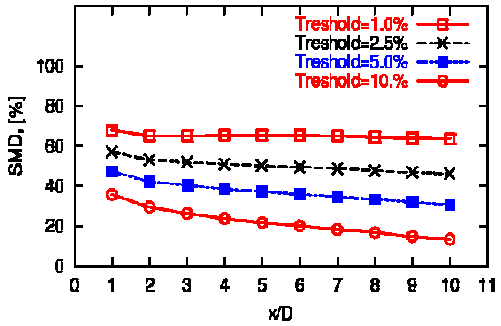

Fig. 4. The SMD mixing index computed with the same four values of the area-defining threshold as used for the TMD.

Reacting scalars. Instantaneous values for the concentration of A in the centerplane are shown in Fig. 5. The "spanwise rollers" at the windward face of the jet (arrow) are responsible for the strong mixing of A and B in this region. Due to the chemical reaction, the scalar A vanishes in the centerplane beyond x/D=5, i.e. $<Y_A>$ drops below 0.02. Correspondingly, the average concentration of B (not shown here) increases in streamwise direction due to the absence of reaction with $<Y_B>$=0.6 at x/D=5. The average concentration of the product P is shown in Fig. 6. The largest value of $<Y_P>$=0.387 in this plane is located at x/D=4.15 and z/D=3.95. It is interesting to note that in the centerplane the region of high product concentration is almost entirely below the middle jet trajectory shown in the same figure. This is consistent with the observations for non-reacting scalars where the maximum concentration line has been found to be below the middle jet trajectory, also [1,2].

Further vortex structures of the flow field which will be referred to later are the "hanging vortices" located on the lateral sides of the jet (see Fig. 9 and 10 below). They are–even in the turbulent case–almost steady [2] and a major source for the counter-rotating vortex pair observed further downstream in planes perpendicular to the mean flow (Figs. 2, 11-13 below).

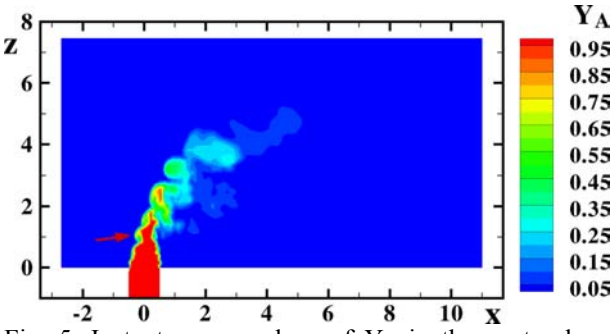

Fig. 5. Instantaneous values of Y_A in the centerplane y/D=0. Here and in the next figures only part of the computational domain is shown.

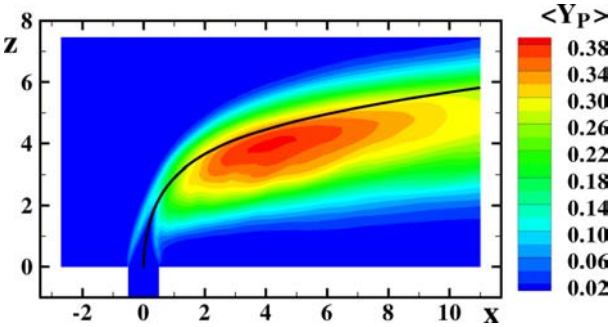

Fig. 6. Average concentration of the product P in the centerplane y/D=0.

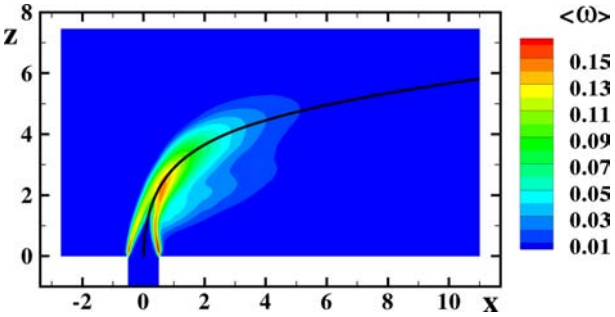

Fig. 7. Averaged reaction rate in the symmetry plane, y/D=0.

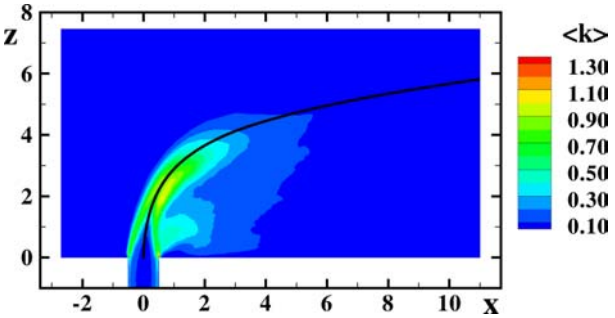

Fig. 8. Average values of the resolved turbulent kinetic energy in the plane y/D=0**.**

The reaction rate ω is used here principally to analyze the mixing process. It is quite a useful quantity for this purpose since being less influenced by the flow development it directly yields information about regions of intense mixing. Fig. 7 presents averaged values of the reaction rate in the plane y/D=0. There are two different regions of high reaction rate in this plane. The first one is located in the upstream mixing layer, where the spanwise rollers contribute to the mixing. The second one is in the downstream mixing layer, where the "hanging vortices" contribute to intensifying of the mixing. The largest value of <ω> in the plane y/D=0 is equal to 0.166; found at x/D=0.5 and z/D=0.2. The absolute maximum of the reaction rate is 0.196 and attained off the centerplane in the hanging vortices at height z/D=0.3.

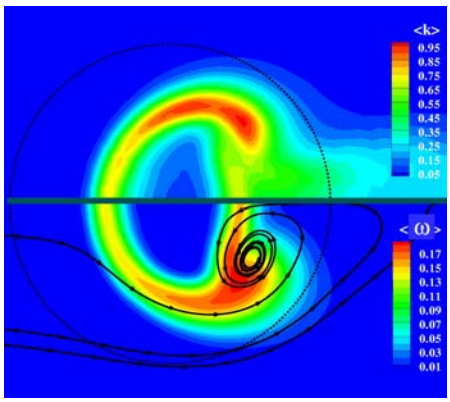

Fig. 9. Average values in the horizontal plane z/D=0.5: a) turbulent kinetic energy (top), b) reaction rate with selected average streamlines included (bottom). The circle shows the position of the pipe. The horizontal axis is the x-axis.

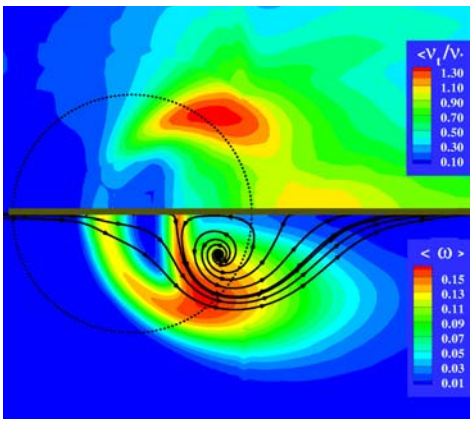

Fig. 10. Average values in the horizontal plane z/D=1: a) reaction rate (top), b) ratio of turbulent to molecular viscosity (bottom). The horizontal axis is the x-axis.

The averaged reaction rate from Fig. 7 has a typical shape of two "tongues". This feature is also present in the average values of the resolved turbulent kinetic energy <k> displayed in Fig. 8. It also features two regions of high values at the same locations as the regions of maximum reaction rate. The high correlation between <ω> and <k> is also observed in wall-parallel planes, at z/D=0.5 in Fig. 9, as well as z/D=1.0 and z/D=2.0 (not shown here). The correlation between <k> and <ω> is not generally observed in all flows but a result of the boundary conditions being imposed, e.g. for the scalars. In the present configuration it is on the other hand quite natural since high values of <k> are related to strong turbulence, in particular resulting from

coherent structures, and correspondingly large turbulent transport $\langle u_i' Y_j' \rangle$ which in turn enhances mixing and reaction.

The bottom part of Fig. 9 and Fig. 10 also shows that close to the outlet the reaction zone is confined to an annular region with no reaction in the center of the jet. Further upwards, the non-reacting zone becomes narrow and flat due to the impact of the hanging vortices visualized by means of selected streamlines of the average flow in this plane. Note, however, that these lines are not average path lines of fluid elements since they constitute the two-dimensional projection from the three-dimensional flow field. The hanging vortices point upwards, almost vertically but inclined towards the lee side of the jet and the flow turns counter-clockwise in the lower part of the pictures. This results in convection of fresh gas towards the jet axis generating a stronger reaction rate at the rear of the jet compared to the front part where it would perhaps be expected. The reaction rate attains its maximum in the plane z/D=0.5 in the outer part of the hanging vortex at an angle of about 45 degrees from the symmetry plane. In the plane z/D=1, the vortex is located closer to the center plane and the reaction zone still at an angle of 45 degrees but further downstream.

As mentioned above, the resolved values of concentration are used to calculate the reaction rate ω. The *a priori* tests in [8] showed that this model leads to an over-prediction of the reaction rate when compared to DNS calculations. This is the more valid the coarser the numerical grid is, i.e. the further away the LES-values appear from the DNS ones. Therefore, the resolution properties of the numerical grid will be addressed now. As a measure of the "relative coarseness" of the grid, the ratio of the averaged turbulent viscosity to molecular viscosity is used. It is according to the authors' experience close to the ratio of average turbulent dissipation to total dissipation proposed in [9] to quantify resolution and errors in an LES. Fig. 10a shows that this ratio is about 1.3 in the region of the hanging vortices and tends to zero in the upstream mixing layer where the spanwise rollers are present (left hand side of the circle). The chemical reaction is hence almost entirely resolved in the upstream mixing layer, as in a DNS, while following [6] the reaction rate near the hanging vortices should be over-predicted.

A salient feature of the jet in crossflow configuration is the counter-rotating vortex pair (CVP) forming downstream of the pipe exit. It is generated by the hanging vortices [2] as well as the upward distortion of vortex rings near the axis in the rear part [1]. The CVP is visualized in Fig. 11 by means of average streamlines in the plane x/D=3. The upward motion in the centerplane brings fresh gas into the interior of the jet which results in stronger mixing than observed with a plane jet [2]. The average concentration of non-reacting scalars for this reason becomes kidney-shaped in planes x=const. as observed in Fig. 2 further downstream at x/D=9. With reactive scalars, the reaction zone roughly exhibits the shape of an 80% circle which is visible in Fig. 11, so that similar to Fig. 9 and 10 the highest reaction rate is reached remote from the symmetry plane. Also note that the absolute maximum of the product concentration $\langle Y_P \rangle$ occurs in this plane, x/D=3, at y=0.79 and z=2.4.

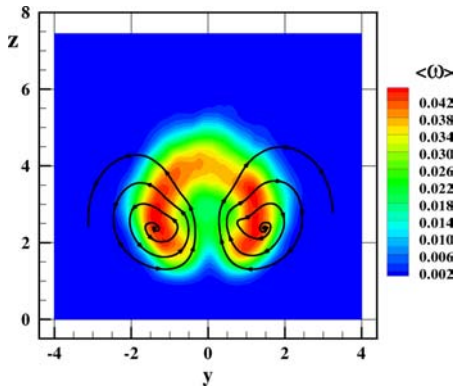

Fig. 11. Average reaction rate $\langle \omega \rangle$ in the plane x/D=3 together with average streamlines in this plane.

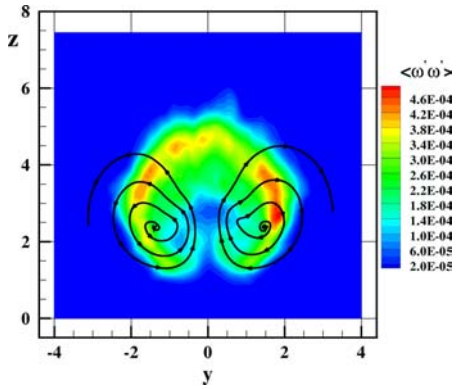

Fig. 12. Fluctuations of the reaction rate $\langle \omega' \omega' \rangle$ in the plane x/D=3.

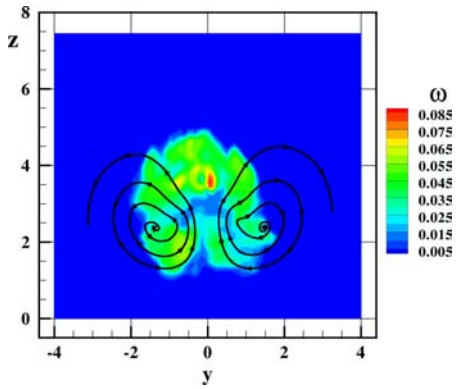

Fig. 13. Snapshot of the instantaneous reaction rate ω in the plane x/D=3.

Fig. 12 shows the average fluctuations $\langle \omega' \omega' \rangle$ in the plane x/D=3. This quantity is smaller in the lower and interior part of the jet, where for a non-reacting scalar the fluctuations are smaller than in the upper part of the jet, because of the mixing during the intrusion of outer fluid into the jet [1,2]. On the other hand $\langle \omega' \omega' \rangle$ is large along the outer border of the reaction zone. This

reflects the strong intermittency of the flow in this region created by coherent structures such as the spanwise rollers and secondary structures resulting from these. To provide an impression of this feature, Fig. 13 displays a snapshot of the instantaneous reaction rate. Reaction takes place in irregularly distributed large pockets with characteristic size of about D at this station. Due to the strong intermittency the fluctuations $<\omega'\omega'>$ take longer time for averaging than other quantities, but the result is already quite clear in Fig. 12.

Conclusions

The mixing process in a jet in crossflow has been investigated by means of LES. A non-reactive passive scalar supplied in the pipe was used for quantification in a first step. The most important outcomes in this respect are:

- The large differences in the jet trajectory for laminar and turbulent jet inflow justifies the additional effort of constructing turbulent boundary conditions in the pipe by means of a precursor simulation with 440 000 additional control volumes.
- Local flow reversal in the pipe and chemical reactions occur with laminar inflow but not with turbulent inflow due to the fuller velocity profile.
- The TMD mixing index was evaluated for planes with increasing x/D coordinate. For the present configuration of a jet in a comparatively wide crossflow no characteristic area for the required averaging is immediately available. Hence, it is suggested here to define this area by means of a threshold for the scalar concentration. The resulting values of the TMD are sensitive to the value of the threshold. But at the same time, the slope of the TMD index is found to be insensitive to the threshold in the present case. It was found that using the TMD in this manner is advantageous over the SMD since with the latter the slope is not insensitive to the area-defining threshold.

The mixing was furthermore studied by means of a single-step chemical reaction. The most important results from this analysis are:

- The flow regions of high reaction rate ω correspond very well with regions of high turbulent kinetic energy reflecting the impact of turbulent mixing on the reaction rate.
- When considering the average concentration of the products P in the symmetry plane it is found that the maximum is below the middle jet trajectory. This observation is consistent with previous work [3,1] where the maximum concentration of a nonreacting scalar was found to be below the middle jet trajectory.
- Both, spanwise rollers and hanging vortices cause an increased value for the reaction rate. The reaction rate is highest in the region of the hanging vortices and the absolute maximum has been found very close to the pipe exit at z/D=0.3.
- Scalar A supplied in the pipe reacts fully within the computational domain. Its average concentration at x/D=5 is less than 0.02.
- The turbulent viscosity has been applied as a measure to assess the numerical grid. It shows that for the present study the numerical grid was fine enough close to the outlet in the region where the spanwise rollers are active and reaction is under-resolved in the region of the hanging vortices and the downstream wake.
- The counter-rotating vortex pair substantially impacts on the reaction rate in planes perpendicular to the mean flow so that the reaction zone forms an incomplete circle. The fluctuations of the reaction rate are large at the outer boundary due to the coherent structures formed in the mixing layer between the jet and the crossflow.

Acknowledgements

The authors acknowledge financial support by the German Research Foundation through the priority Programme SPP-1141 “Analysis, Modeling and Computation of Mixing devices with and without Chemical Reactions”.

References

[1] J. Fröhlich, J.A. Denev, H. Bockhorn, in: P. Neittaanmäki, T. Rossi, K. Majava, and O. Pironneau (eds.), W. Rodi and P. Le Quéré (assoc. eds.), Proc. of the 4th European Congress on Computational Methods in Applied Sciences and Engineering, ECCOMAS 2004, July 24-28, Jyväskylä, Finland, vol.1. (2004) CD-ROM.

[2] L. L. Yuan, R. L. Street, J. H. Ferziger, J. Fluid Mech. 379 (1999) 71-104.

[3] L. L. Yuan, R. L. Street, Phys. Fluids, 10(9) (1998) 2223-2335.

[4] C. Hinterberger. Dreidimensionale und tiefengemittelte Large-Eddy-Simulation von Flachwasserströmungen, PhD thesis, Institute for Hydromechanics, University of Karlsruhe, 2004.

[5] H. Werner, H. Wengle, in: F. Durst, R. Friedrich, B.E. Launder, F. W. Schmidt, U. Schumann, J.H: Whitelaw (eds.), Selected papers from the 8th Symposium on Turbulent Shear Flows Springer, 1993, 155-168.

[6] P. E. DesJardin, S. H. and Frankel, Phys. Fluids 10 (9) (1998) 2298-2314.

[7] J. Boss, Bulk Solid Handling 6(6) Dec (1986) 1207-1215.

[8] C. Prière, L.Y.M. Gicquel, P. Kaufmann, W. Krebs, T. Poinsot, J. Turbulence 5 (2004) 005, 1-24.

[9] B.J. Geurts, J. Fröhlich, Phys. Fluids, 14 (2002) L41-L44.